APPLIED PHYSICS LETTERS **88**, 011908 (2006)

Epitaxy of nonpolar AlN on 4H-SiC (1-100) substrates

R. Armitage, J. Suda,[a] and T. Kimoto
Department of Electronics Science and Engineering, Kyoto University, Nishikyo-ku, Kyoto Daigaku-Katsura, Kyoto 615-8510, Japan

(Received 1 August 2005; accepted 4 November 2005; published online 4 January 2006)

AlN has been grown on 4H-SiC (1-100) substrates by rf-plasma molecular beam epitaxy. The epilayers assume a metastable 4H structure to match the in-plane stacking arrangement of the substrate. Initial two-dimensional nucleation of 4H-AlN is revealed by reflection high-energy electron diffraction. The epitaxial quality is evidenced by narrow x-ray diffraction ω-scan linewidths less than 70 arcsec for both symmetric and asymmetric reflections. The AlN growth surface exhibits a smooth and anisotropic morphology similar to that of GaN (1-100). Large residual stress is present in the epilayers, consistent with incomplete relaxation of misfit strain during growth. © *2006 American Institute of Physics*. [DOI: 10.1063/1.2161809]

GaN epilayers with (1-100) and (11-20) orientations[1–5] are of interest because these orientations avoid the undesirable effects of built-in electric fields[6] prevalent in light-emitting devices fabricated on the typically used polar (0001) orientation. However, the quality of nonpolar GaN epilayers is still inferior to that of state-of-the-art GaN (0001) epilayers, and basic questions remain unanswered, such as which nonpolar orientation, (1-100) or (11-20), should offer better growth characteristics. Prior work on nonpolar nitride growth has focused mainly on GaN, but sufficient attention should also be given to nonpolar AlN since deep-ultraviolet devices requiring active layers of high Al content are most effectively fabricated on AlN templates.[7] Hardly any data have been published for AlN (1-100); one study[8] mentioned that this orientation could be grown on 6H-SiC (1-100) substrates, but did not describe the epilayer material properties. In this letter we focus on the growth of AlN (1-100).

Growth experiments were performed in an EV-1000S molecular-beam epitaxy chamber (Eiko Engineering Ltd. Japan) equipped with Al and Ga effusion cells and an Applied Epi rf nitrogen source. The 4H-SiC (1-100) substrates were supplied by SiXON Ltd. (Japan) and were subjected to high-temperature gas etching[9] to remove polishing damage. The substrates were cleaned in 3:1 H_2SO_4/H_2O_2 and 0.5% HF solutions prior to loading into the vacuum chamber. Three cycles of Ga deposition and desorption[10] were applied as a further *in situ* cleaning process. Subsequently, the substrate was exposed to the nitrogen plasma beam for 5 min at 950 °C. AlN growth was then initiated by opening the Al shutter. The rf source was operated at 400 W and 1 sccm which gave a N-limited growth rate of 8 nm/min based on postgrowth thickness measurements. The Al beam-equivalent pressure was optimized at 8×10^{-7} Torr corresponding to the transition between Al-droplet and droplet-free growth regimes. The AlN thickness studied ranged from 40 to 720 nm.

Since the atomic stacking sequence lies inside the growth plane for nonpolar orientations of the wurtzite structure, the generation of stacking faults at the interface may be a serious problem in epitaxy of nonpolar nitride layers on nonisomorphic substrates. However, for AlN on 4H-SiC (11-20) a metastable 4H phase of AlN could be obtained,[5] resulting in isomorphic growth and significantly reduced epilayer defect densities. In the present work it is demonstrated that metastable 4H-AlN layers can similarly be grown on 4H-SiC (1-100) substrates. The 4H-AlN (1-100) layers exhibit improved growth characteristics compared to previously reported 4H-AlN (11-20) layers.[5]

During the initial stages of AlN growth on 4H-SiC (1-100), reflection high-energy electron diffraction (RHEED) intensity oscillations are clearly observed as shown in Fig. 1. The oscillation period of 2.1 s is in good agreement with the time (2.0 s) required for deposition of 1 ML of (1-100) AlN at the growth rate of 8 nm/min. Since intensity oscillations would not occur for a defective 2H/4H interface, this result implies successful 4H polytype replication. The 4H structure of the AlN layer is confirmed by the geometries of the RHEED patterns. Figure 2 shows RHEED patterns along the ⟨11−20⟩ azimuth before and after growth of a 250 nm AlN layer. The atomic periodicity in this direction differs by a factor of 2 for 4H-SiC and 2H-AlN. However, the streak spacing of the AlN layer is almost identical to that of 4H-SiC, thus AlN grew in the 4H structure. RHEED patterns showing 4H symmetry are observed for AlN growth thick-

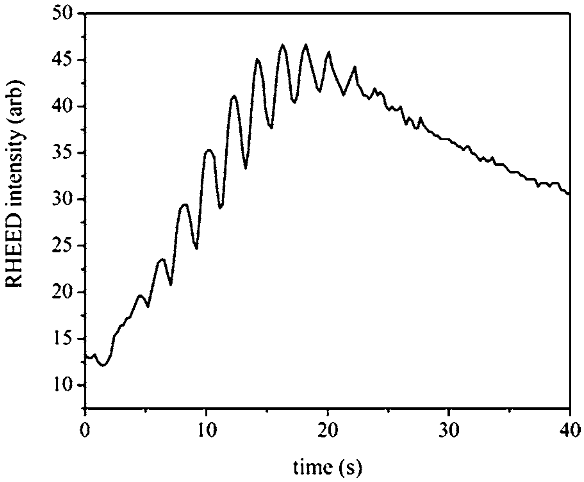

FIG. 1. Intensity of specular RHEED diffraction streak as a function of AlN growth time ([0001] azimuth). Oscillations were also observed for [11-20] and [11-23] azimuths.

---

[a] Present address: Japan Science and Technology Agency (JST), Kawaguchi, Saitama 332-0012, Japan; electronic mail: suda@kuee.kyoto-u.ac.jp

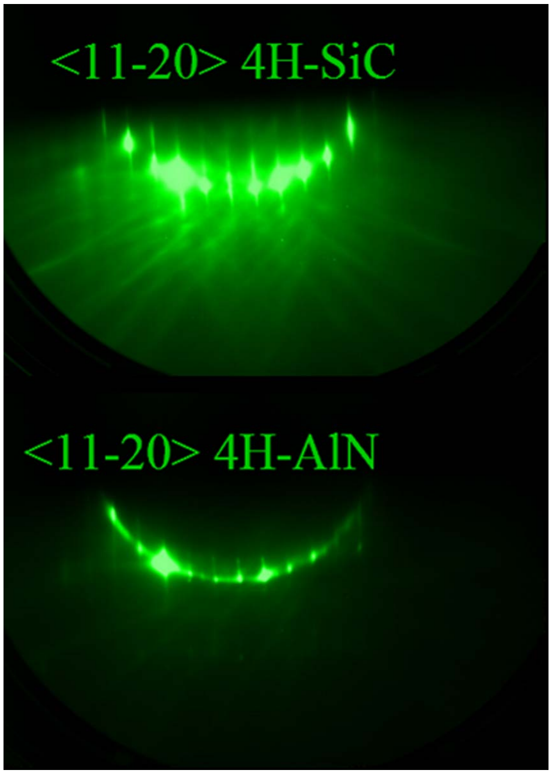

FIG. 2. (Color online) RHEED patterns ([11-20] azimuth) from 4H-SiC substrate (top) and after growth of 250 nm AlN (bottom).

ness up to at least 250 nm, although there is evidence for mixing of 2H and 4H phases in thicker layers. The band gap of the AlN layers determined by reflectivity at 300 K is ~5.9 eV. This value might be expected for the 4H polytype if the relationship E_g 3C(5.7 eV) $<E_g$ 4H $<$ E_g 2H(6.2 eV) is assumed to hold for AlN.[11]

The RHEED patterns of AlN layers grown under optimal conditions exhibit weak half-order reconstruction streaks along all azimuths except ⟨11−20⟩ after cooling to ~800 °C. This corresponds to the Al/N flux ratio near the transition point above which Al droplets are formed. The 1×2 reconstruction vanishes upon exposure to the nitrogen plasma beam, implying that it is related to Al adatoms. For higher values of the Al flux the reconstruction streaks are more intense and can even be observed during growth at 950 °C, however for such high Al/N flux ratios droplets are formed on the layer surfaces. If it is assumed that the observed AlN 1×2 reconstruction is analogous to that of the GaN (1-100) surface,[4] then the optimal AlN growth conditions can be associated with an Al surface coverage of 1–2 ML.

The AlN lattice relaxation process for optimized conditions was evaluated from the time dependence of the RHEED streak spacings along the ⟨0001⟩ and ⟨11−20⟩ azimuths (Fig. 3). The in-plane *a*-lattice constant begins to relax at a thickness <1 ML and reaches a constant value after ~7 ML. However, the constant value reached (~0.311 nm) is smaller than the *a*-lattice parameter expected for bulk AlN at 950 °C (~0.312 nm), suggesting incomplete misfit relaxation. The *c*-lattice relaxation data suffer from a poor signal-to-noise ratio because the ⟨11−20⟩ streak spacing is not very much larger than the streak width. The AlN *c*-axis data scatter around the *c*-lattice parameter of the SiC substrate and do not show any downward trend. This suggests that within experimental resolution, the *c*-lattice constant of AlN remains equal to that of the SiC substrate for a layer thickness up to at least 14 ML.

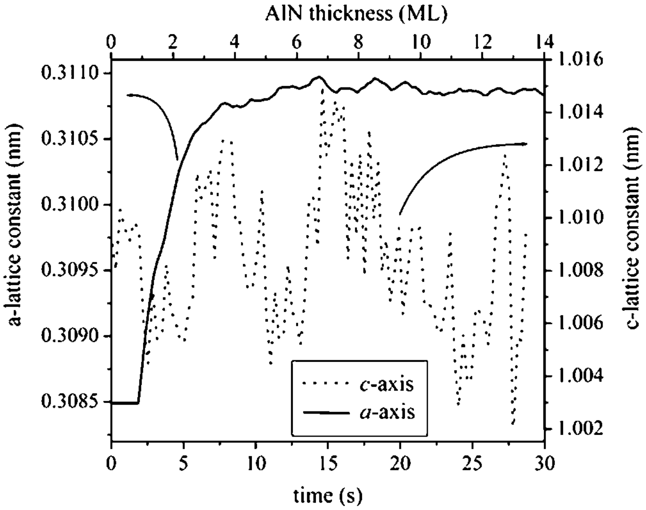

FIG. 3. Lattice relaxation process for AlN on 4H-SiC (1-100) determined from variations of [11-20] and [0001] RHEED streak spacings with AlN growth time. 4H-SiC reference values (950 °C) taken as $a=0.3085$ nm, $c=1.0094$ nm.

Atomic force micrographs for a representative 250 nm epilayer are shown in Fig. 4. The root-mean squared (rms) roughness is ~0.9 nm and the AlN morphology is characterized by stripe features parallel to ⟨11−20⟩, similar to (1-100) GaN grown by molecular-beam epitaxy.[4] The stripe-feature density of the present (1-100) epilayers is $\sim10^5$ cm^{-1}, while that of (11-20) 4H-AlN was $\sim10^6$ cm^{-1}.[5] An order of magnitude lower basal plane stacking fault density in the (1-100) AlN layers is therefore implied if the stripe features are assumed to be directly related to such faults.[3]

The AlN structural quality has been assessed by high-resolution x-ray diffraction (XRD). Both the symmetrical and asymmetrical reflections of the epilayers exhibit narrow ω-scan peaks, as shown in Fig. 5. Full width at half maximum (FWHM) values as small as those shown in Fig. 5 have been successfully reproduced over several AlN growth runs.

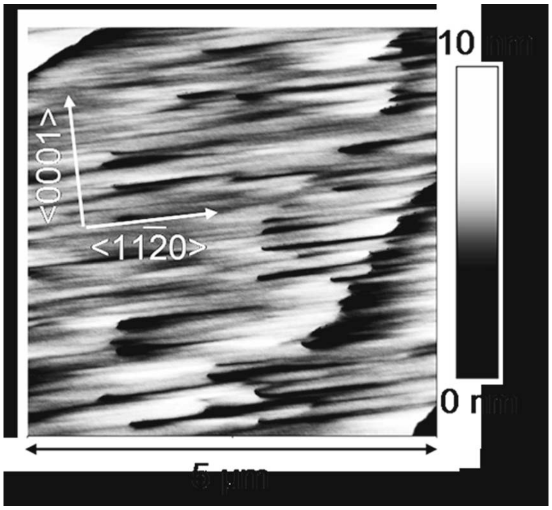

FIG. 4. A 5×5 μm^2 atomic force microscopy scan for 250 nm AlN on 4H-SiC (1-100). *Z* range 0–10 nm.

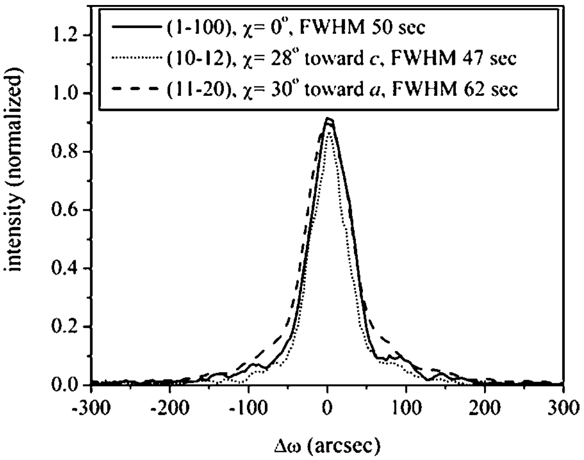

FIG. 5. X-ray (1-100), (10-12), and (11-20) ω scans for 250 nm AlN on 4H-SiC(1-100).

The symmetric ω-scan FWHM values for optimized AlN epilayers do not change when measurements are made for different orientations of the incident x-ray beam with respect to the sample c axis.

Significant residual strain exists in the AlN layers after growth. Although layers less than about 300 nm thick are crack free, cracks running along {0001} planes are observed by optical microscopy for thicker layers. Cracking can be attributed to the combination of tensile residual misfit stress and differences in thermal expansion ($\Delta\alpha=-0.6\times10^{-6}$/K, Ref. 12) along the c axis. From XRD $2\Theta-\omega$ scans the lattice parameters of a 250 nm crack-free layer were calculated as $a_1=0.3097$ (parallel to the epilayer surface), $a_2=0.3111$ (inclined 30 ° with respect to the surface normal), and $c/2=0.4998$ nm. Compared to bulk AlN ($a=0.3112$, $c=0.4980$ nm) these values indicate the presence of residual strains too large to attribute to differences in thermal expansion alone. The misfit strain was not completely relaxed.

In summary, AlN has been found to assume a metastable 4H structure when grown on 4H-SiC (1-100) under optimized conditions. With two-dimensional AlN initial nucleation, XRD ω-scan FWHM values smaller than 70 arcsec for both symmetric and asymmetric reflections, as well as a rms surface roughness <1 nm over a 5 μm^2 area, were obtained. While other issues must be considered, e.g., the presence of stacking faults and the nontransparency of the SiC substrate, these results suggest that 4H-AlN (1-100) may be a useful template for fabrication of deep-ultraviolet light-emitting devices free from the effects of internal polarization fields.

[1] P. Waltereit, O. Brandt, A. Trampert, H. T. Grahn, J. Menniger, M. Ramsteiner, M. Reiche, and K. H. Ploog, Nature (London) **406**, 865 (2000).
[2] H. M. Ng, Appl. Phys. Lett. **80**, 4369 (2002).
[3] B. A. Haskell, F. Wu, M. D. Craven, S. Matsuda, P. T. Fini, T. Fujii, K. Fujito, S. P. DenBaars, J. S. Speck, and S. Nakamura, Appl. Phys. Lett. **83**, 644 (2003).
[4] O. Brandt, Y. J. Sun, L. Däweritz and K. H. Ploog, Physica E (Amsterdam) **23**, 339 (2004).
[5] N. Onojima, J. Suda, T. Kimoto, and H. Matsunami, Appl. Phys. Lett. **83**, 5208 (2003).
[6] S. F. Chichibu, A. C. Abare, M. S. Minsky, S. Keller, S. B. Fleischer, J. E. Bowers, E. Hu, U. K. Mishra, L. A. Coldren, S. P. DenBaars, and T. Sota, Appl. Phys. Lett. **73**, 2006 (1998).
[7] J. P. Zhang, M. Asif Khan, W. H. Sun, H. M. Wang, C. Q. Chen, Q. Fareed, E. Kuokstis, and J. W. Yang, Appl. Phys. Lett. **81**, 4392 (2002).
[8] S. Stemmer, P. Pirouz, Y. Ikuhara, and R. F. Davis, Phys. Rev. Lett. **77**, 1797 (1996).
[9] S. Nakamura, T. Kimoto, H. Matsunami, S. Tanaka, N. Teraguchi, and A. Suzuki, Appl. Phys. Lett. **76**, 3412 (2000).
[10] R. Kaplan and T. M. Parrill, Surf. Sci. Lett. **165**, L45 (1986).
[11] V. Cimalla, V. Lebedev, U. Kaiser, R. Goldhahn, Ch. Foerster, J. Pezoldt, and O. Ambacher, Phys. Status Solidi C **2**, 2199 (2005).
[12] L. Liu and J. H. Edgar, Mater. Sci. Eng., R. **37**, 61 (2002).